CILAMCE 2017
Florianópolis - Santa Catarina - Brazil

PREDICTING CASING FAILURE IN PRE-SALT WELLBORES USING ARTIFICIAL NEURAL NETWORKS

Anna Luiza de C. Santos

Fernanda L. G. Pereira

Deane M. Roehl

annaluiza@tecgraf.puc-rio.br

nandalgp@tecgraf.puc-rio.br

deane@tecgraf.puc-rio.br

Department of Civil Engineering and Tecgraf Institute, Pontifical Catholic University, Marquês de São Vicente 225, Gávea, RJ 22451-900, Brazil

Abstract. *Brazilian pre-salt wellbores are characterized by the presence of salt rocks, such as Halite, which has elasto-viscoplastic time-dependent behavior. Throughout the lifetime of a wellbore, salt expands under creep effects. Faults in cementation inside the annular may allow the salt to reach the casing, creating plastic regions as a consequence of high localized stresses, indicating wellbore failure. This work proposes a numerical model with a fault in cementation (no cement in the annular), in which there is a casing/salt contact, leading to well failure. It is also considered a 2D plane-strain analysis in a quarter symmetry. An artificial neural network is used to obtain an equation for the casing failure through the von Mises criterion. The network receives as input five physical parameters of the model: Young modulus, Poisson coefficient, initial stress state, drilling mud pressure and Halite deformation rate. These input data are original from fifty models, carried out in Abaqus. The results of the analyses are the elapsed times for yielding in each model, which are used to feed the network. The neural network was trained with fifty numerical models as input data, each composed by five varying parameters and one output. The best architecture found was 5-2-1, reaching a 99 percent accuracy level in the results, predicting very well the yielding times for the casing.*

Keywords: *Artificial neural networks, Casing failure, Pre-salt wellbore, Finite element method, Cementation failure*

1 INTRODUCTION

Cementation failures are very common in wellbores due to construction difficulties at certain well depths, the fluid cement cannot be properly pumped and the annulus is not completely filled. In the cementation process interruptions caused by natural phenomena may enable these gaps between casing and salt. Willson et al. (2003) assesses the problem of salt loading on well casings, and provides a historical examination of the experimental and numerical analyses on this issue. The lack of cement in the annular creates a problem for the integrity of the wellbore, once it exposes the surface of the casing to the salt rock. Since most boreholes are not perfectly circular, the closure rate is not uniform. Subsequently, salt will affect a sector of the casing, resulting in nonuniform loading. This contact can generate plastic zones in the casing, leading to well failure.

Previous works have studied cementation faults and their effects on borehole closure. Fossum et al. (2007) carried out a probabilistic analysis to determine the time it takes the casing to yield once salt has contacted the casing. A finite element model coupled with a reliability method was developed to perform those analyses. This numerical model was adapted by Firme et al. (2012) in order to reduce the distortion in the mesh elements. In their study, a probabilistic analysis determined which parameters of the formation were determining for the yielding of the casing. Several other works referred to casing design under nonuniform salt loadings, such as Cheatham et al. (1964) and Hackney (1985).

Artificial neural networks (ANNs) are a useful tool to make predictions and evaluate risks in engineering problems. In oil engineering fields, amongst several other scientific applications, ANNs can be applied to obtain prompt answers, circumventing the traditional numerical modeling worflows and eventually reducing the overall cost of projects. Sadiq et al. (1998) used neural networks to predict the frictional drag and transmission of slack-off in horizontal wells; Sadiq et al. (2000) predicted the formation fracture gradient; Pereira et al. (2014) applied ANNs to estimate the maximum allowable injection pressure in order to prevent fault reactivation.

In this work, a neural network is implemented to create a model to predict the casing lifespan considering material integrity. The network is trained with synthetic data provenient from numerical modeling, using the finite element method. Through the knowledge of only five physical parameters of the problem, the expected time for the induction of plastic deformations in the casing is determined. Once the ANN is succesfully trained, the output can be obtained through an equation, without the necessity of a numerical analysis, reducing the overall computational cost. This also eliminates the necessity of prior knowledge about the problem in order to gain the wanted information. The user won't have to be a specialist in the field on numerical and constitutive models. The only information required to use the neural network are the five input parameters.

2 PROBLEM DESCRIPTION

2.1 Creep deformations

When salt formation is drilled, by removing part of the material, dress unloading around the borehole occurs. Salt starts to deform progressively, under constant stress and temperature.

Since salt is governed by creep behavior, consequently its displacements are time-dependent, so it's important to verify the integrity of the well throughout its lifetime and not only instantaneously. The multi-mechanism (MM) deformation creep model is adopted as the constitutive model for the Brazilian Halite in this work. It is based on the superposition of three microscopic mechanisms of creep and represents well both the transient and steady-state phases in the salt rock. For more information on the MM creep model, calibration parameters and its formulation see previous work by Firme et al. (2012).

2.2 Failure condition

The contact between casing and formation is very likely to happen, and even though it is not an impediment to the construction of the well, it should be investigated. When salt deformation leads to contact with the formation, stresses are introduced. The contact between salt and casing does not occur uniformly, due to the fact that certain points of the casing surface are closer to the salt than others. Consequently, the loading is nonuniform.

In Fig. (1), stage (1) represents the moment when salt has not yet reached the casing. In stage (2), the first contact between casing-salt happens. In stage (3) the first plastic region appears. Eventually, salt reaches all casing surface, as shown in stage (4). As a consequence of this, loading becomes uniform and some of the plastic regions experience stress relief. The

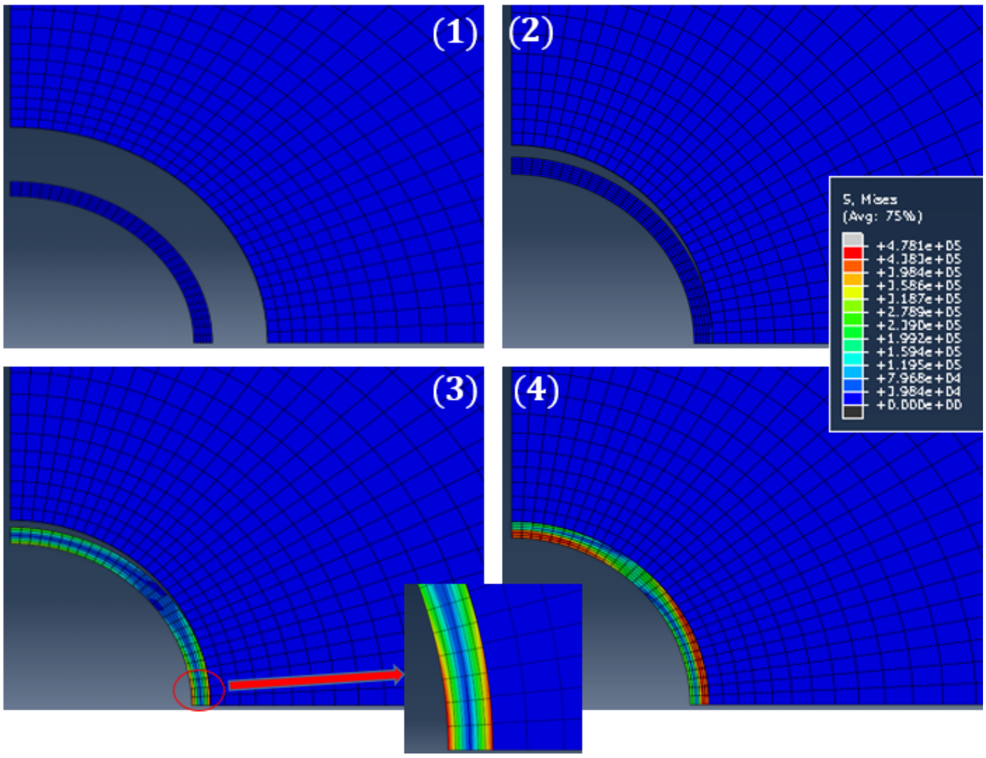

Figure 1: Contact between casing and salt

plastic ratio for the steel casing is equal to the reason between the applied stress over the von Mises stress. Once this ratio in any point of the casing exceeds the unit value, it is considered that the well has failed. For this reason, the important result to be extracted from the analysis is the first instant for which a plastic region is generated.

3 METHODOLOGY

Five parameters were chosen as the input for the network: Young modulus E_h, Poisson coefficient υ_h, initial stress state σ_h and deformation rate $\dot{\varepsilon}_0$ of the salt rock (Halite) and drilling mud pressure P_{flu}. In the work by Firme (2012) they were also presented as the most influential random variables on the casing yielding, through a probabilistic analysis. The elastic parameters are responsible for the instantaneous deformation after drilling, and influence also in the creep curve, according to the constitutive model. After drilling, the difference in stresses increase due to the geostatic and mud pressure applied, acting directly on the creep deformations. The deformation rate determines how creep will act on the salt rock, which affects directly the time for first contact and subsequent the plastic deformation of the casing.

A summary of the workflow adopted in this work is illustrated in Fig. (2).

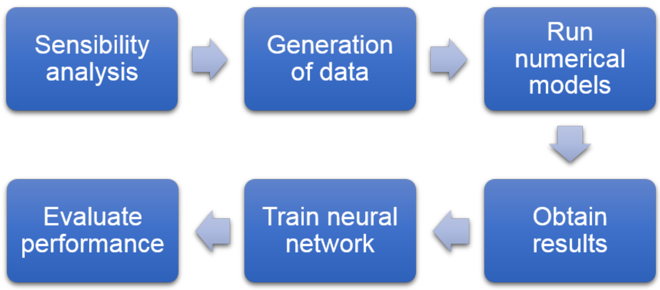

Figure 2: Workflow of the methodology adopted in this work

At first, a sensitivity study was necessary to determine the suitable ranges for each parameter. Several analysis for each variable were carried out to adjust the applicable extents.

Fifty different samples were created as a random yet continuous combination of the five parameters. All values inside the established ranges had the same probability to appear in the combinations. The software Nessus was used to generate these values under the structured Monte Carlo method, and further combining variables among themselves, creating the individuals for training. A routine was implemented to alter the entry files with such parameters in Abaqus.

The next step was to run all fifty numerical models in Abaqus. Once all the analyses were carried out, a routine in Java ran though the results file of each model. It looked for the first of any the four gauss points in each steel element that presented a tension equal or bigger to the von Mises tension for steel and collected the correspondent time.

To train the neural network, a routine in Matlab was implemented, with all input and output data. Matlab offers its own platform to work with neural networks: The neural network toolbox. In order to train the network in Matlab, the user has to introduce the input and output variables and choose amongst the several algorithms available, which will be used. After succesful training, outputs were retrieved and compared against the original, assessing the network's performance.

4 NUMERICAL MODEL

4.1 Geometry

The geometric model proposed in this paper represents the borehole, casing and salt rock, portrayed in a plane-strain analysis, in a quarter symmetry. In the extension considered no cement is present in the annular. The borehole presents ovalization of five percent in its diameter. The numerical model was first implemented by Fossum et al.(2007) and later on by Firme et al.(2012), where the mechanical properties of the salt were substituted by a brazilian salt rock and it was developed with a circular outer border, in order to have elements with low levels of distortion, resulting in quadrangular elements yet with quadratic displacements. The finite element mesh is composed of 2745 quadratic plane strain elements, with a 2x2 reduced integration.

4.2 Material properties and boundary conditions

The borehole is cased by a steel casing, modeled as an elastic perfectly plastic material and the Halite as an elasto-viscoplastic material. The constitutive model adopted for the Halite was the Multi-mechanism model, implemented via Fortran subroutine by Firme (2012), as a plugin into the ABAQUS software. The contact between casing and salt is modeled by the master-slave strategy. The whole geometric model has a diameter of forty meters, about eighty-five times the size of the outer diameter of the wellbore, discarding possible border effects. The outer boundaries of the model are constrained in both x and y directions, preventing displacements, as shown in Fig. (3).

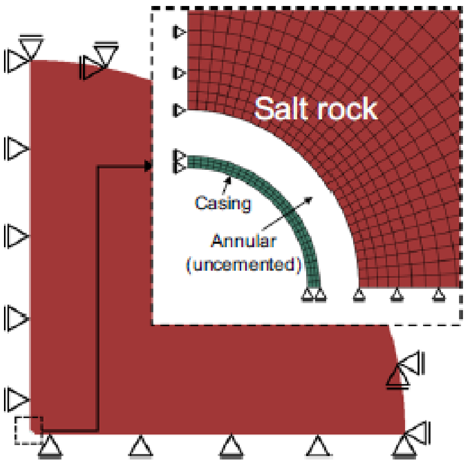

Figure 3: Geometry of the model and boundary conditions (Firme, 2016)

4.3 Applied loads

The spacing in the annulus and the inside part of the borehole are filled with drilling fluid, acting as pressures on such surfaces (inner and outer casing). Since only a certain depth is being considered (2d plane analysis) the formation is assumed to be under an initial stress state, equal to the weight of the overburden at the specified depth. The whole model is considered to be under uniform temperature conditions.

The stages of the model construction are illustrated in Fig. (4). In the “Formation” stage, the geostatic load is applied on the model. Then, in the “Drilling” stage, the formation is excavated instantly to construct the borehole, creating a free surface inside the original salt surface. At this point, the drilling pressure is applied and creep starts to act on the Halite. Between the “Drilling” and “Liner” stages, there is a period of 120 hours (five days), where the salt rock is under only creep effects, and starts to expand. After this period, the liner is created in the model, also in an instantaneous step. The final phase is the creep analysis through the expected wellbore lifespan of thirty years. During this period the salt formation expands and may touch the casing, as shown in “Contact Liner-Salt” stage.

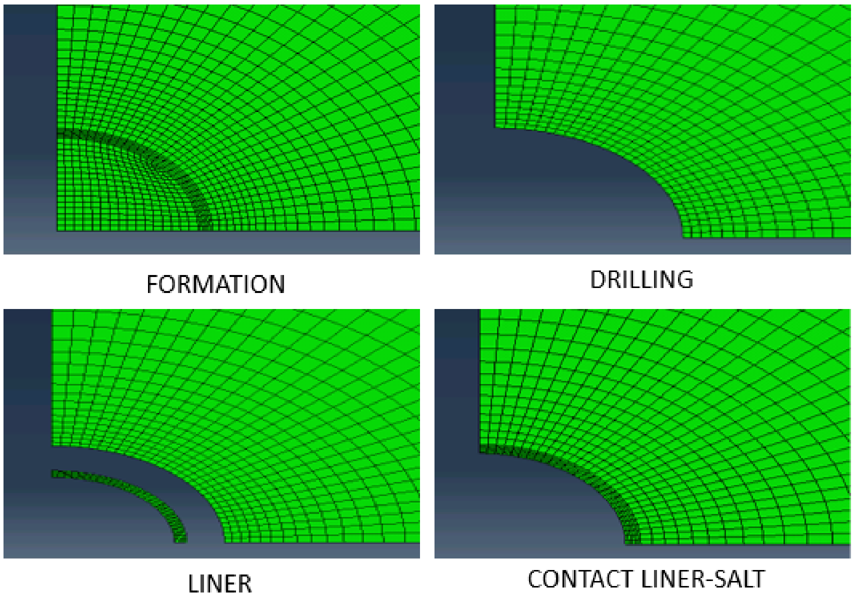

Figure 4: Stages of the model

5 ARTIFICIAL NEURAL NETWORKS

5.1 Main characteristics and applications

Computational intelligence is a powerful tool, such as machine learning, deep learning and decision trees, to optimize the gathering of results in several fields of research. Nowadays, its branches are employed to generate prompt response surfaces for complex problems. Artificial neural networks are widely used in pattern recognition, sample categorizing and value prediction problems. The algorithm and architecture of the network are based on the human brain and nervous system, on how it is organized and the way it processes information, specifically in its capacity to learn with experience.

The neural network is capable of mastering the behavior of a problem through a sample of individuals, each one with inputs and outputs. This way, the network can capture the relationship between them, even if its physical meaning is not well understood. By this premise, with only a few parameters of the problem, the network is able to preview with sufficient accuracy the final answer, without the necessity of providing all the information. This can be achieved due to its great generalization power.

The use of neural networks escapes the traditional methods, because it requires previous knowledge about the problem. We can classify the ANN as an optimization tool to obtain results, not as an isolated tool to collect them. It can be a great way to deal with expensive models and problems with great variability, hard to predict. Neural networks have as prime abilities the processing of information through logical and arithmetical functions; transformation of independent variables into dependent ones; parallel data processing and nonlinear analysis. It can also be applied in cases where the data is imprecise or incoherent. According to the work by Fausett (1994), ANNs have the capability of approximating any nonlinear complex function between input and output parameters.

5.2 Multilayer perceptron

The multilayer perceptron network is one of the most used and simplest types of ANNs available. A typical architecture for a perceptron, as shown in Fig. 5, consists of at least three layers. The first layer consists of the entry parameters neurons. The hidden layers contain the neurons, and the output layer has as many neurons as the number of outputs of the network. Each entry datum is associated with a vector of synaptic weights, transmitted as an entry signal to each neuron in the network.

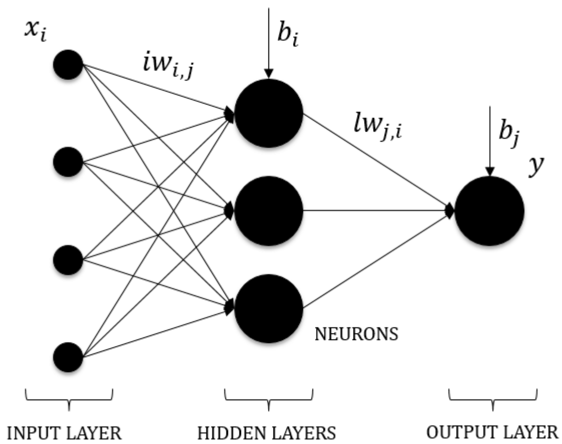

Figure 5: Typical neural network architecture

The neurons are responsible for processing the information and transmitting it to the neuron in the next layer. Each neuron receives an entry signal: the input data x_i multiplied by its synaptic weight ($iw_{i,j}$ for the hidden layers and $lw_{j,i}$ for the output layer), plus the bias value (b_i for the hidden layers and b_j for the output layer). According to the activation function (or transfer function) adopted in the layer, it returns the output signal y. The number of input parameters corresponds to i,the number of neurons to j.

The learning phase is described by Haykin (1999). It consists of the calibration of the synaptic weights to their best possible values, following the generalized delta rule, as shown in Eq. (1), where α is the momentum constan, δ_j is the local grandient, η is the learning rate and n

is the corresponding neuron. In each iteration the network comes to an output answer, and the process continues until the minimum error is achieved.

$$\Delta w_{ij}(n) = \alpha \Delta w_{ji}(n-1) + \eta \delta_j(n) y_i(n) \tag{1}$$

The feedforward-backpropagation method (with mean-squared error selected as a performance function), is adopted in this paper. The feedforward learning function goes through the entire network from beginning to end (entry to output). The error is calculated at the end and is propagated in the inverse direction, multiplying the previous synaptic weights, altering their values (backpropagation). The Levenberg-Marquardt is chosen as training function and the Gradient descent with momentum weight and bias is the learning function.

The mean-squared-error (MSE) is adopted as the error condition, as shown in Eq. (2), where n is the number of neurons, y is the output and $y^{'}$ is the target.

$$MSE = \frac{1}{n} \sum_{i=1}^{n} (y - y^{'})^2 \tag{2}$$

The transfer function for the intermediate layer is the logistic-sigmoid, shown in Eq. (3), where $v_j(n)$ is the induced local field of neuron j and a is an adjustable positive parameter.

$$\varphi_j(v_j(n)) = \frac{1}{1 + e^{-av_j(n)}} \tag{3}$$

The output transfer function is the purely linear, shown in Eq. (4).

$$\varphi_j(v_j(n)) = v_j(n) \tag{4}$$

To determine the prime architecture of the network several models were tested in increasing level of complexity. Starting from only one hidden layer with one neuron, mantaining a nonlinear activation function for the intermediate layers (logistic-sigmoid), with a linear function for the output layer (widely-employed in prediction value models). The number of neurons were incremented as the performance of the network improved, until reaching convergence. The same process was adopted for the number of layers, and dispersion of neurons throughout layers.

5.3 Entry parameters

To construct the sampling space to feed the network we need individuals that contain the data of the problem, which can come from different sources: experimental works, actual field data or provenient from numerical analyses. As previously described in Section 4, the data used to train this network are synthetic, in another words they had to be generated by the user.

Prior to training, the data were treated, normalizing entry and output values (from 0 to 1), according to Eq. (5), due to the difference in the order of magnitude amongst them. Y_{min} is the lower bound (zero), Y_{max} is the upper bound (one), X_{min} is the minimum input parameter and X_{max} is the maximum input parameter. In this way, we eliminate the possibility of a parameter dominating the problem due to its larger values, or its importance being undermined for having very small values compared to the others. The ranges for each input parameter used in training are displayed in Table (1).

$$\frac{Y - Y_{min}}{Y_{max} - Y_{min}} = \frac{X - X_{min}}{X_{max} - X_{min}} \tag{5}$$

Table 1: Ranges for each input parameter

Input parameter	Nomenclature	Lower value	Upper value
Young modulus (GPa)	E_h	17.5	32.8
Poisson coefficient	v_h	0.10	0.39
Initial stress state (MPa)	σ_h	83.1	84.9
Deformation rate ($10^{-6}s^{-1}$)	$\dot{\varepsilon}_0$	1.88	2.19
Drilling mud pressure (MPa)	P_{flu}	63.0	64.9

5.4 Training

The fifty samples were separated randomly in three classes: seventy percent for training, fifteen percent for validation and fifteen percent for testing. This is a default setting in Matlab, and is highly recommended to avoid overfitting. The training samples are responsible for the calibration of the synaptic weights. Validation samples, even though they do not participate in the training phase, determine the prime epoch to stop training, which happens when the mean-squared-error reaches minimum value. The values of the weights and biases will be collected in this iteration. The testing samples will be responsible for verifying the performance of the network, in order to predict responses outside training, comparing the target to the actual output.

6 RESULTS

The best architecture was chosen as the one which presented the minimal medium error, as Fig. (6) shows. It contains only one hidden layer, with log-sigmoid activation function for the two neurons in it.

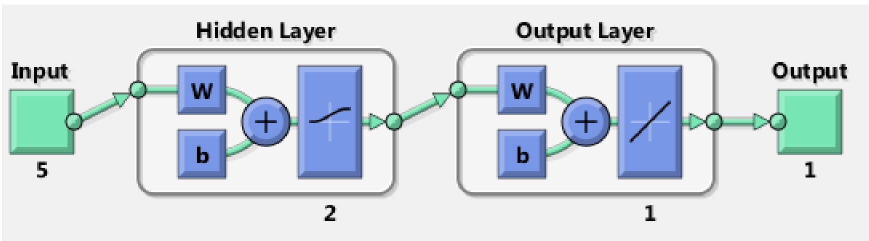

Figure 6: Neural network architecture

An indication of good performance is the evolution of the error for both test and validation samples. It is important that they present a similar behavior over the epochs. If this does not occur, it can indicate a bad division of samples or even an excessive number of neurons. The best validation performance occurs at epoch 25, according to the performance graph, shown in Fig. (7). This graph shows the evolution of the error between target and output of the network, over each iteration or epoch. The prime epoch is chosen as the one where the validation samples present the minimum mean squared-error.

The network had excellent results, reaching over 99 percent accuracy for training samples, as shown in Fig. (8). Comparing the target values to the outputs provided by the network, we

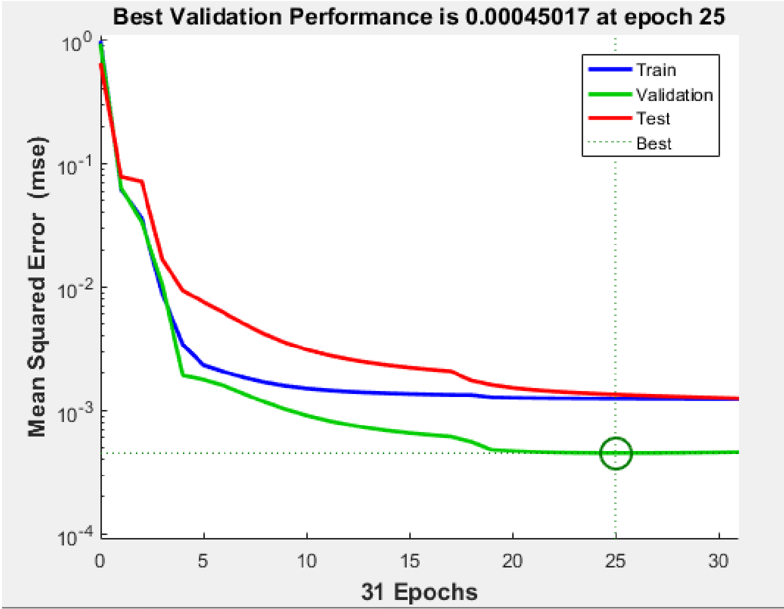

Figure 7: Evolution of the MSE over the number of epochs

can evaluate the error for each class of samples. When $R = 1$, it means that the network has given as output the exact same value as the target solution. Test samples present a 98,9 percent precision in results, which is considered a excellent result.

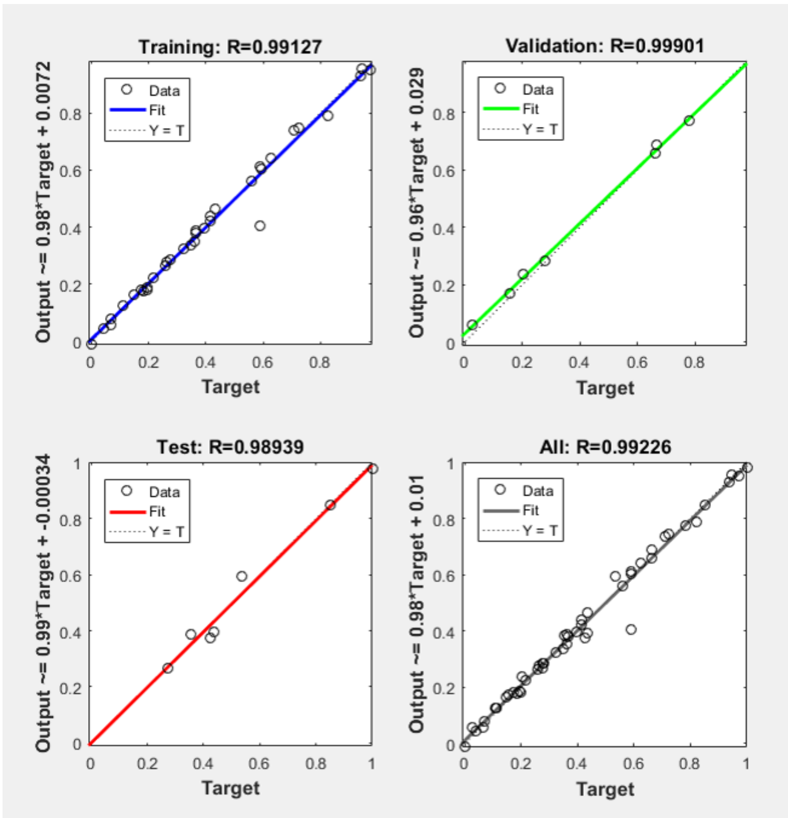

Figure 8: Comparison between output values and target values

After training, a final equation for the output can be obtained, considering the transfer functions adopted, synaptic weights and bias values, according to Eq (6) and Table (2).

$$Output = y = lw \times \frac{1}{1+e^{-n}} + b_2 \tag{6}$$

Where

$$n = \begin{bmatrix} \sum_{i=1}^{5} iw_{1i} \cdot x_i + b_1(1) \\ \sum_{i=1}^{5} iw_{2i} \cdot x_i + b_1(2) \end{bmatrix}$$

and

$$x = \begin{bmatrix} x_1(\dot{\varepsilon}_0) \\ x_2(E_h) \\ x_3(v_h) \\ x_4(\sigma_h) \\ x_5(P_{flu}) \end{bmatrix}$$

Table 2: Synaptic weights and bias values

Nomenclature	Value
iw	$\begin{bmatrix} 0.5232 & -2.2229 & 1.2379 & 2.5235 & 0.9353 \\ -0.2462 & 0.0926 & 0.2029 & -0.5308 & 0.6681 \end{bmatrix}$
b_1	$\begin{bmatrix} -1.7634 \\ -0.8812 \end{bmatrix}$
lw	$\begin{bmatrix} -0.2423 & 4.3769 \end{bmatrix}$
b_2	-1.4522

7 CONCLUSIONS

This paper presents a casing failure problem in pre-salt wellbores combining artificial neural networks and the finite element method. The ANN technique is adopted to establish the casing lifespan through the knowledge of five parameters of the problem. The data sets used for training the network are provenient from fifty numerical analyses, carried out in Abaqus.

A model for the neural network was implemented, capable of generalizing the results very well. The ANN becomes an interesting alternative for the finite-element modelling. It is a useful and efficient tool for obtaining fast and accurate response-surfaces for complex problems.

A 5-2-1 architecture was adopted, providing 99 percent accuracy in results. This architecture can change, requiring a higher level of complexity (more neurons and layers) if more individuals are used for training, or even more than five parameters are adopted as entry data. Another factor that contributes to the quality of results is that only physical parameters were varied, maintaining all other characteristic information fixed: such as loading, discretization of time, finite-element mesh, and the model geometry.

As the sampling space grows, the network gathers more information and can provide better results. Since the objective of this work was to optimize the time to obtain results, this model is adequate and fifty samples were more than sufficient.

ACKNOWLEDGMENTS

This work was supported by the National Council for Scientific and Technological Development (CNPQ) and Brazilian Petroleum S.A. (Petrobras). This support is gratefully acknowledged.

REFERENCES

Willson, S.M.& Fossum, A.F. & Fredrich, J.T. 2003. *Assessment of salt loading on well casings*, SPE Drilling Completion Vol 18, pp. 1321.

Fossum, A.F. & Fredrich, J.T. 2007. *Probabilistic analysis of borehole closure for through-salt well design*, Acta Geotechnica Vol 2, pp. 41-51.

Firme, P. 2012. *Modelagem Constitutiva e Análise Probabilística Aplicadas a Poços em Zonas de Sal*, Master's dissertation, PUC-Rio.

Firme, P. & Roehl, D. & Romanel, C. 2016. *An assessment of the creep behaviour of Brazilian salt rocks using the multi-mechanism deformation model*, Acta Geotechnica, Vol 11, pp. 1445-1463.

Cheatham, J.B.Jr. & McEver, J.W. 1964. *Behavior of Casing Subjected to Salt Loading*, JPT 1069, Trans., AIME, 231.

Hackney, A.M. 1985. *A New Approach to Casing Design for Salt Formations*, SPE/IADC 13431.

Sadiq, T. & Gharbi, R. 1998. *Prediction of Frictional Drag and Transmission of Slack-off Force in Horizontal Wells Using Neural Networks*, SPE 51083.

Sadiq, T. & Nashawi, I. S. 2000. *Using Neural Networks for Prediction of Formation Fracture Gradient*, SPE/Petroleum Society of CIM 65463.

Pereira, L. C. & Guimares, L.J.N. & Horowitz, B. & Snchez, M. 2014. *Coupled hydro-mechanical fault reactivation analysis incorporating evidence theory for uncertainty quantification*, Computers and Geotechnics Vol 56, pp. 202-215.

Fausett, L.V. 1994. *Fundamentals of Neural Network: Architecture, Algorithm, and Application*, New Jersey: Prentice Hall.

Haykin, S. 1999. *Neural Networks and Learning Machines*, 3rd ed.